

Study on Multipactor Breakdown in Coaxial to Microstrip Transitions

Miguel A. Sánchez-Soriano¹, Stephan Marini¹, Joaquin Vague², Celia Gómez³, Fernando Quesada³, Alejandro Álvarez³, Vicente E. Boria² and Marco Guglielmi²

¹Department of Physics, Systems Engineering and Signal's Theory, University of Alicante, Carretera de San Vicente, 03690 Alicante, Spain

²iTEAM, Universitat Politècnica de València, Camino de Vera s/n, 46022 Valencia, Spain

³Universidad Politécnica de Cartagena, Campus Muralla del Mar s/n, 30202 Cartagena, Spain

Email: m.sanchez.soriano@ieee.org, smarini@ua.es

Abstract—The objective of this paper is to study multipactor breakdown in coaxial to microstrip transitions. This kind of transitions generally exhibit a gap just below the central pin of the coaxial connector. This gap can create a region where the electric fields are relatively strong so that an electron path may be created that could potentially lead to a multipactor breakdown. In this paper, we study the multipactor modes which may be induced as a function of structural parameters, such as the substrate thickness and the gap length. In particular, it is found that two kinds of electron trajectory can be created leading to critical power levels that are even lower than those obtained with the parallel-plate model, generally used as a conservative model. In this context, we demonstrate that multipactor breakdown can happen for input power levels lower than 500 W. This, in turn, may become a critical issue for the use of classic coaxial to microstrip transitions in new high power satellites whenever payloads are manufactured using planar technology.

Index Terms—coaxial to microstrip transition, high power applications, multipactor, power breakdown threshold.

I. INTRODUCTION

Currently, space communication systems provide a large number of services to our modern Digital Society. Future space communications will offer data transmission through mega clusters of Low Earth Orbit (LEO) micro-satellites, with moderate to high power handling capabilities (up to 1 kW), and higher component integration. The use of planar technology will, therefore, be essential. In this context, multipactor breakdown [1], [2], namely, an electron avalanche discharge occurring in vacuum, still remains a critical problem. The effects of a multipaction avalanche can vary from the degradation of the communication channel, to the total destruction of the device. For this reason, multipactor is considered as a critical issue in the design of medium to high power microwave space components [3], [4].

The study of RF breakdown in shielded microstrip lines has recently attracted much interest in the space research community. This is because of the higher power levels recently reached by Solid State Power Amplifiers (SSPAs) based on microstrip circuits [5]. Previous studies [6] reveal that microstrip

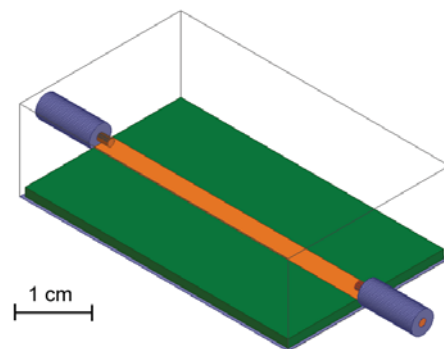


Fig. 1. 3D view of the implemented matched microstrip line under study.

circuits are strongly resistant to multipactor discharge due to the presence of fringing fields, which prevent the creation of well defined electron paths in the structure. However, connectors, bridges and ribbons have also been analyzed [7], [8], demonstrating that, in some cases, multipactor avalanche is indeed possible.

The objective of this paper is to go one step further and investigate in detail the multipactor breakdown in the coaxial to microstrip interface. It is shown that, depending on the geometry of the transition, different multipactor modes can be induced, if a gap is present in the interface, leading to relatively low critical power threshold levels. The detailed features of this transition, therefore, become an important issue that must be taken into account from the very beginning in the satellite design and manufacturing process.

II. DESCRIPTION AND ANALYSIS

To study multipactor breakdown, we first focus our attention on a matched microstrip line implemented using a conventional substrate, such as Rogers RO4003 ($\epsilon_r = 3.55$, substrate thickness $h = 1.52$ mm, conductor layer thickness $t = 18$ μm and loss tangent $\tan \delta = 0.002$). Fig. 1 shows the 3D view of the matched line enclosed in a metal housing (only the edges are shown for the sake of clarity), where the coaxial to

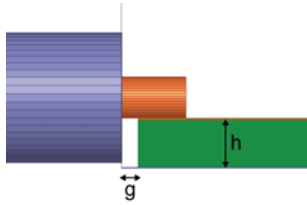


Fig. 2. Lateral view of the coaxial to microstrip transition.

microstrip transition can be also seen. The coaxial connector has a pin diameter of 1.28 mm, an outer diameter of 4.06 mm, and uses Teflon as a dielectric. The microstrip line width is 3.4 mm. This kind of transition generally leads to the generation of a gap g between the metal housing and the dielectric substrate, as shown in Fig. 2. This gap creates a region below the coaxial pin where the electric fields are relatively strong so that an electron trajectory may be defined which can potentially lead to a multipactor discharge. For this to happen, the following conditions must be met: 1) synchronization between the transient time along the electron trajectory and the electric field oscillations; and 2) the kinetic energy of the electrons must be high enough to create secondary electron emission impacting on the surfaces surrounding the gap in the structure. The first condition can be expressed as

$$\omega t = n\pi + \alpha \quad (1)$$

where ω is the angular frequency, t is the transient time of the electrons along the path, n is the multipactor order and α is a reference phase. The second condition is basically modeled by the Secondary Electron Yield (SEY) of the surfaces involved.

In this work, all multipactor simulations have been performed using the commercial software tool SPARK3D^{®1}. This tool uses the real electromagnetic field distribution of the device under test (coming from a full-wave simulator), to solve numerically the motion equations, as defined by the Lorentz' force, of a number of seed electrons assumed to be present in the structure. The SEY of all surfaces involved in the structure is fully taken into account. The software predicts very accurately the electron trajectories in the time domain, and the power levels at which an electron avalanche (multipactor phenomenon) can occur in the device.

The analysis is performed both at L-band and at S-band, at 1.6 GHz and 3.0 GHz, respectively. The first case analyzed is an ideal connector attachment, i.e., $g = 0$ mm. For this case, the only region where multipactor can happen is between the top (metallic) layer of the substrate and the top inner face of the metal housing, as already been studied in [6]. The fringing fields of microstrip lines make the creation of a well defined electron path in this region virtually impossible. As a consequence, microstrip circuits (with an ideal connector attachment) are very resistant to multipactor effect. This

¹SPARK3D, Copyright (C) 2012-2013 AuroraSat, available on <http://www.cst.com/products/spark3d>

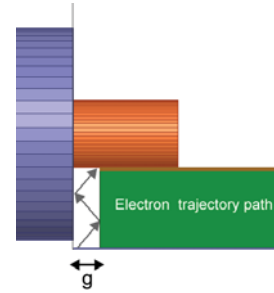


Fig. 3. Lateral view of the coaxial to microstrip transition where the electron trajectory path for low values of g can be observed.

TABLE I
MAXIMUM POWER THRESHOLD FOR $h = 1.52$ MM. AT 1.6 GHz.

g (mm)	Power threshold (W)	Multipactor Order
0.1	> 10,000	–
0.3	425	1
0.5	287	1
1.0	605	1
1.5	960	1
2.5	992	1

TABLE II
MAXIMUM POWER THRESHOLD FOR $h = 1.52$ MM. AT 3.0 GHz.

g (mm)	Power threshold (W)	Multipactor Order
0.1	> 10,000	–
0.3	138	1
0.5	1,980	1
1.0	4,300	2
1.5	6,400	2
2.5	7,900	2

conclusion has been also corroborated by the results of our simulations.

Tables I and II show the simulated results, at both frequencies, for different values of g . At both frequencies, there is no multipactor for $g < 0.1$ mm for power levels up to 10 kW, which is far above the levels of normal microstrip applications. This is due to the fact that with a gap so small, the free electrons undergo too many bounces, as well as multiple collisions with each other during their motion, thus, multipactor resonance is completely blocked.

For $0.1 < g < 1.0$ mm, our simulations indicate that the electrons follow a well defined zig-zag trajectory between the central pin of the connector and the bottom ground plane of the housing, as shown in Fig. 3. The minimum power threshold is found for $g = 0.5$ mm at 1.6 GHz, and for $g = 0.3$ mm at 3.0 GHz. This result seems logical since both situations give the same frequency \times distance product. It is important to note that the threshold values identified indicate that there may be problems in using this coaxial to microstrip transition for space applications with power levels reaching 1 kW.

For $g > 1$ mm, the electron trajectories follow a vertical

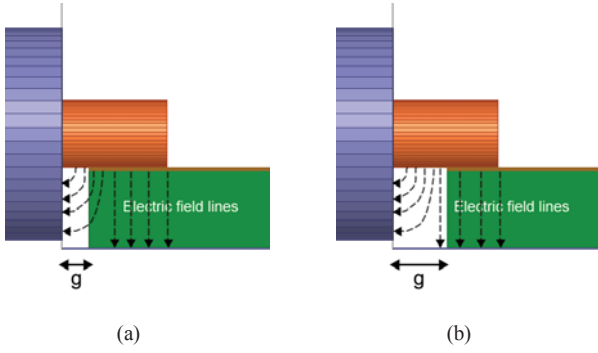


Fig. 4. Electric field lines below the connector pin. a) For low values of g . b) For $g > 1.0$ mm.

path between the pin and the housing ground. This trajectory is very similar to the one produced in the parallel-plate model, which is usually used to provide conservative power thresholds. In fact, the power threshold levels we obtain at 1.6 GHz for $g > 1$ mm are close to the ones given by the parallel-plate model for a distance between plates of 1.52 mm. At 3.0 GHz, for $g > 1.0$ mm, the power threshold levels are considerably higher than those at 1.6 GHz. This is because of the higher $f \times d$ value, which makes the resonance condition for a multipactor verified for an order higher than 1.

At this point, it is interesting to study the difference between the two kinds of electron trajectories which appear as a function of g . For this, it is convenient to see how the electric field is distributed inside the gap. Fig. 4 shows the electric field lines for two different g values. For g lower than h , the electric field lines along the gap are rather parallel to the connector pin than vertical, since the lateral ground is closer to the pin (and to the microstrip) than the bottom ground. However, if g increases, the vertical electric field lines predominate along the gap. This effect, along with the fact that for lower g values the collisions with the walls are easier, can explain the two kinds of electron trajectories. This result is important, since the zig-zag multipactor mode leads to power threshold levels lower than those obtained with the parallel-plate model.

III. COMPARISON BETWEEN DIFFERENT SUBSTRATE HEIGHTS

The same study has also been carried out also for substrates with lower thickness values. In this case, the substrate used is again RO4003, but with $h = 0.813$ mm. Tables III and IV show the simulated results at 1.6 GHz and 3.0 GHz. The power threshold levels obtained in our simulations are lower than those obtained in the previous cases. This is due to the lower $f \times d$ value. An important difference with respect to the thicker substrate analyzed in Section II is that, with a thinner substrate, the zig-zag electron trajectory does not appear for any value of g . The reason for this is that, for thinner substrates, the ratio h/g makes the electric field lines be predominately vertical along the gap, leading to vertical trajectories for the electrons. Fig. 5 shows the multipactor power threshold at 1.6 GHz for the two matched lines under analysis (i.e., for the two different

TABLE III
MAXIMUM POWER THRESHOLD FOR $h = 0.813$ MM. AT 1.6 GHz.

g (mm)	Power threshold (W)	Multipactor Order
0.1	> 10,000	–
0.3	108	1
0.5	93	1
1.0	76	1
1.5	88	1

TABLE IV
MAXIMUM POWER THRESHOLD FOR $h = 0.813$ MM. AT 3.0 GHz.

g (mm)	Power threshold (W)	Multipactor Order
0.1	> 10,000	–
0.3	480	1
0.5	628	1
1.0	652	2
1.5	726	2

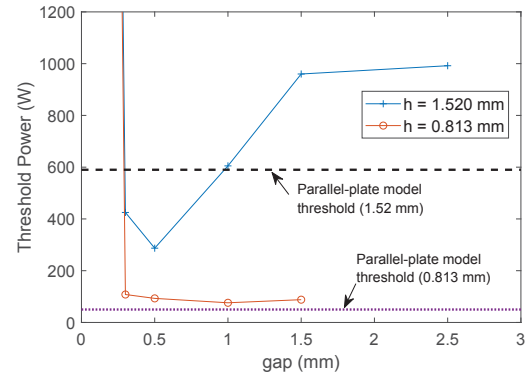


Fig. 5. Multipactor power thresholds at 1.6 GHz as a function of g for the two substrates under analysis.

substrates) as a function of g . In this figure, we have also plotted the thresholds obtained with the parallel-plate model. As we can see, the zig-zag multipactor mode, happening for $h = 1.52$ mm in the range $0.3 < g < 1.0$ mm, leads to power threshold levels lower than those of the parallel-plate model. For $h = 0.813$ mm, the multipactor power thresholds converge to the parallel-plate model for $g > 0.5$ mm.

In view of the above results, we can clearly see that the classic lateral coaxial to microstrip transition can drastically limit the power handling capability of microstrip circuits for space applications. This transition, however, is very commonly used because it is very easy to be implemented from a technological point of view. A possible solution to overcome this drawback could be to fill completely the gap with a dielectric material. This, however, may be technologically hard to implement. More research work is clearly needed in this critical area.

IV. CONCLUSIONS

In this paper, we investigate in detail the multipactor breakdown of classical coaxial to microstrip transitions using a full-wave simulation tool. Our findings indicate that a multipactor mode can indeed be induced below the connector pin, leading to rather low power thresholds. The specific electron trajectory of the multipactor mode induced has been found to be different depending on the substrate height, and the ratio between the thickness and the gap. Our work indicates that two kind of trajectories can be identified, namely, zig-zag and vertical. The multipactor breakdown thresholds linked to the vertical trajectory are similar to the values of the parallel-plate model, whereas the zig-zag trajectory may result in power thresholds that are lower than those predicted by the parallel-plate model. The low power thresholds found for some of the cases studied pose a severe limit on the use of this very popular transition for next generation satellites, where power levels are expected to approach the value of 1 kW.

ACKNOWLEDGMENTS

This work has been supported by the “Agencia Estatal de Investigación (AEI)” and by the EU through the “Fondo Europeo de Desarrollo Regional -FEDER- Una manera de hacer

Europa (AEI/FEDER, UE)”, under the coordinated research project TEC2016-75934-C4, and by the University of Alicante under the research project GRE16-17.

REFERENCES

- [1] J. Vaughan, “Multipactor,” *IEEE Transactions on Electronic Devices*, vol. 35, pp. 1172–1180, Jul. 1988.
- [2] A. J. Hatch and H. B. Williams, “Multipacting modes of high frequency gaseous breakdown,” *Physical Reviews*, vol. 112, pp. 681–685, Nov. 1958.
- [3] M. Yu, “Power-handling capability for RF filters,” *IEEE Microwave Magazine*, vol. 8, pp. 88–97, Oct. 2007.
- [4] R. J. Cameron, C. M. Kudsia, and R. R. Mansour, *Microwave Filters for Communication Systems: Fundamentals, Design and Application*. New Jersey: John Wiley & Sons Wiley-Interscience, 2007.
- [5] F. J. Perez, S. Anza, M. Mattes, and et. al., “Rigorous investigation of RF breakdown effects in high power microstrip passive circuits,” *Proc. IEEE MTT-S Int. Microwave Symp. Dig.*, pp. 833–836, Jun. 2009.
- [6] V. E. Semenov, E. I. Rakova, A. G. Sazontov, and et. al., “Simulations of multipactor thresholds in shielded microstrip lines,” *Journal of Physics D: Applied Physics*, vol. 42, pp. 1–7, 2009.
- [7] F. J. Perez, F. Quesada, A. Alvarez, and et. al., “Accurate software tool for the prediction of RF breakdown in microwave transmission lines,” *Proc. European Conference on Antennas and Propagation (EUCAP2009)*, pp. 114–118, Mar. 2009.
- [8] F. J. Perez, S. Anza, M. Mattes, and et. al., “RF breakdown analysis in microstrip structures,” *Proc. International Workshop on Multipactor; Corona and Passive Intermodulation (MULCOPIM2011)*, pp. 1–7, Sep. 2011.